# Revisiting the contribution of ATR-FTIR spectroscopy to characterize plant cell wall polysaccharides

Xuwei Liu, Catherine M.G.C. Renard, Sylvie Bureau, Carine Le Bourvellec

Version of Record: https://www.sciencedirect.com/science/article/pii/S0144861721003222
Manuscript_e2efc31663fd0ecc28253bdb110de926

# Revisiting the contribution of ATR-FTIR spectroscopy to characterize plant cell wall polysaccharides

Xuwei Liu[a], Catherine M.G.C. Renard[a, b], Sylvie Bureau[a], Carine Le Bourvellec[a, *]

[a]INRAE, Avignon University, UMR SQPOV, F-84000 Avignon, France

[b]INRAE, TRANSFORM, F-44000 Nantes, France

**Corresponding author***

Carine Le Bourvellec (carine.le-bourvellec@inrae.fr)

INRAE, UMR408 SQPOV « Sécurité et Qualité des Produits d'Origine Végétale »

228 route de l'Aérodrome

CS 40509

F-84914 Avignon cedex 9

Tél: +33 (0)4 32 72 25 35

**Other authors**

Xuwei Liu: xuwei.liu@inrae.fr

Catherine M.G.C Renard: catherine.renard@inrae.fr

Sylvie Bureau: sylvie.bureau@inrae.fr

1

# Graphical Abstract

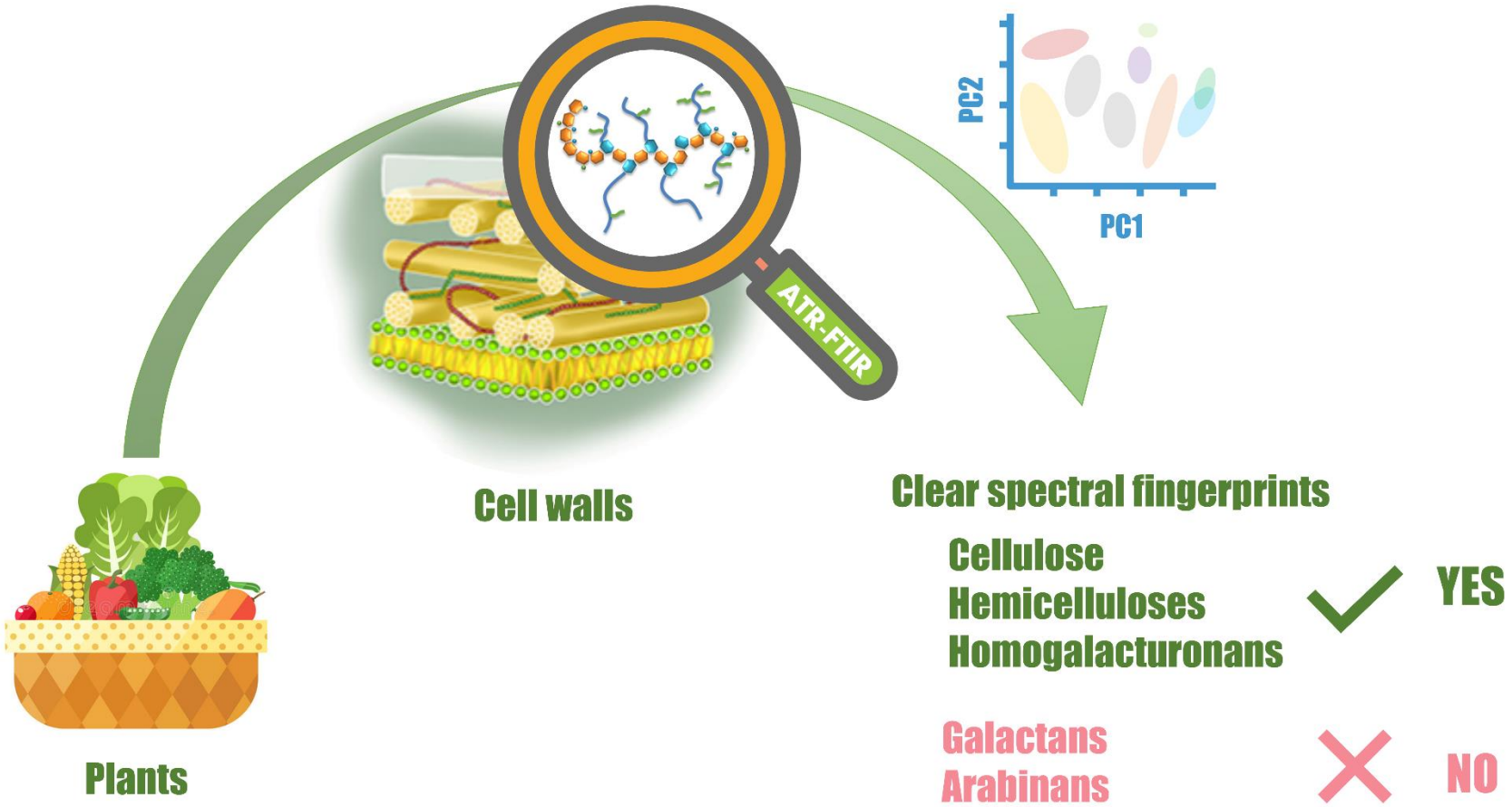


2

**Abstract**

The contribution of ATR-FTIR spectroscopy to study cell wall polysaccharides (CWPs) was carefully investigated. The region 1800-800 $cm^{-1}$ was exploited using principal component analysis and hierarchical clustering on a large range of different powders of CWPs based on their precise chemical characterization. Relevant wavenumbers were highlighted for each CWP: 1035 $cm^{-1}$ was attributed to xylose-containing hemicelluloses, 1065 and 807 $cm^{-1}$ to mannose-containing hemicelluloses, 988 $cm^{-1}$ to cellulose, 1740 and 1600 $cm^{-1}$ to homogalacturonans according to the degree of methylation. Some band positions were affected by macromolecular arrangements (especially hemicellulose-cellulose interactions). However, as arabinan and galactan did not reveal distinctive absorption bands, ATR-FTIR spectroscopy did not allow the discrimination of cell walls differing by the abundance of these polysaccharides, e.g., those extracted from apple and beet. Therefore, the application of ATR-FTIR could remain sometimes limited due to the complexity of overlapping spectra bands and vibrational coupling from the large diversity of CWP chemical bonds.

**Keywords:** ATR-FTIR; Polysaccharides; Cell walls; Cellulose; Pectins; Hemicelluloses

**Abbreviations:**

AIS, alcohol insoluble solids; ATR-FTIR, Attenuated Total Reflectance Fourier Transform Infrared Spectroscopy; DW, dry weight; PCA, Principal Component

Analysis; HCA: Hierarchical Cluster Analysis.

## 1. Introduction

Plant cell walls of the primary walls of dicots and non-grass monocots are dynamic and ordered networks of natural carbohydrate polymers, constituted by an amorphous matrix mainly composed of pectins embedded in a network of cellulose and hemicelluloses, as well as minor amounts of structural glycoproteins, phenolic compounds and enzymes (Carpita, Sabularse, Montezinos, & Delmer, 1979). Cell walls are highly variable according to species, developmental and maturity stages, plant organs and environmental conditions (Anderson & Kieber, 2020; Burton, Gidley, & Fincher, 2010). Therefore, this makes it difficult to easily identify and quantify cell wall components.

In general, the structure and composition of plant cell walls are characterized after sample extraction, pretreatment (e.g., acid hydrolysis) and diverse specific biochemical analyses (e.g., chromatography, mass spectrometry, spectrophotometry), which are expensive and time-consuming. An advanced tool based on mid-infrared spectroscopy would provide the advantages of rapid and easy analysis of the prepared samples. Attenuated Total Reflectance Fourier Transform Infrared Spectroscopy (ATR-FTIR) has been increasingly used for the rapid characterization of cell walls of fruits and vegetables (Chylinska, Szymanska-Chargot, & Zdunek, 2016; Coimbra, Barros, Barros, Rutledge, & Delgadillo, 1998; Coimbra, Barros, Rutledge, & Delgadillo, 1999; Ferreira, Barros, Coimbra, & Delgadillo, 2001; Kacurakova, Capek, Sasinkova, Wellner, & Ebringerova, 2000; Szymanska-Chargot, Chylinska, Kruk, & Zdunek, 2015). Especially in recent years, it has become a powerful research

technology to clarify the composition of dry carbohydrate samples (Canteri, Renard, Le Bourvellec, & Bureau, 2019). This method appears really convenient insofar as it avoids undesirable structural changes that may occur during sample analysis, e.g., extraction and preparation. Moreover, ATR-FTIR can detect changes in the fruit and vegetables during processing at the cell wall level (Lan, Renard, Jaillais, Leca, & Bureau, 2020).

The identification of cell wall polysaccharides by infrared spectroscopy is generally carried out on the different polysaccharide fractions obtained by sequential extractions (the extraction of pure polysaccharides is imperfect), followed by ethanol precipitation and anion exchange chromatography. These extracted polysaccharides are then characterized using chemical and biochemical methods (Brahem, Renard, Gouble, Bureau, & Le Bourvellec, 2017; Coimbra et al., 1999; Renard, 2005; Szymanska-Chargot et al., 2015; Szymanska-Chargot & Zdunek, 2013). However, these studies do not use purified polysaccharides to confirm the absorption bands identified by comparison with the literature. Moreover, some studies have also performed polysaccharide analysis using spectral data but obtained from KBr pellets or aqueous solutions, the classical way before the development of the ATR method (Kacurakova et al., 2000). Fruits and vegetables are highly hydrated and susceptible to environmental conditions. Drying, not only prevents samples from oxidation and hydrolysis under the action of endogenous enzymes, but also concentrates samples by water elimination, so it significantly improves the reflectance spectra of some specific components present in lower content than water (Lan et al., 2020). Therefore, the

systematic analysis of purified solid materials from cell wall polysaccharides by ATR-FTIR may improve their identification.

Moreover, some challenges exist due to the ATR-FTIR response of the different cell wall polysaccharides. For example, according to our previous research, in spite of very different structures and compositions, apple and beet cell walls were poorly discriminated by Principal Component Analysis (PCA) based on ATR-FTIR spectra (Liu, Renard, Rolland-Sabaté, Bureau, & Le Bourvellec, 2021). Therefore, we need to reconsider these results, knowing that the interactions between the internal components of the cell walls (Le Bourvellec & Renard, 2012; Liu, Le Bourvellec, & Renard, 2020) may affect the absorption of these very complex mixtures. This study combined ATR-FTIR and stoichiometry to characterize the abundance and composition of cell wall polysaccharides, taking into account the heterogeneity and interactions between different cell wall components. To track the characteristic peaks of each cell wall component, spectral data and conventional chemical methods are used to study the composition of cell walls and internal structures. In order to evaluate the available information based on extracted samples, powders of cellulose, hemicelluloses, and pectins were also scanned in ATR-FTIR. To identify the typology of the cell walls, both PCA and Hierarchical Cluster Analysis (HCA) were performed. This study provided new explanations and experimental ideas for studying complex natural polymer systems, and guidance for using ATR-FTIR data to clarify carbohydrate structures, physical properties and interactions.

## 2. Materials and methods

## 2.1. Monosaccharide and polysaccharide samples

Monosaccharides (D-(+)-Arabinose, D-(−)-Fucose, D-(+)-Xylose, D-(+)-Mannose, L-Rhamnose, D-(+)-Glucose, and D-(+)-galactose) and D-(+)-Galacturonic acid monohydrate were obtained from Fluka (Buchs, Switzerland). Arabinan (sugar beet), linear 1,5-α-L-arabinan (sugar beet), debranched arabinan, galactan (potato), rhamnogalacturonan I (from potato pectic fibre), and rhamnogalacturonan (from soybean pectic fibre), xylan, arabinoxylan, glucomannan, and xyloglucan were provided from Megazyme (Bray, Ireland). Commercial apple and citrus peel pectins (degrees of methylation ~75%), microcrystalline cellulose and poly-galacturonic acid were provided by Sigma-Aldrich (Deisenhofen, Germany). Homogalacturonan DM 70 was supplied by Watrelot et al. (2013). The common names of cell wall components and their abbreviations used in this study are presented in Table 1.

Native and modified cell walls and pectins from apple, beet and kiwifruit were supplied and characterized by Liu et al. (2021). The native cell wall samples were named as apple cell wall (ACN), beet cell wall (BCN), ripe kiwifruit cell wall (KCRN) and overripe kiwifruit cell wall (KCON), and samples after boiling at pH 2.0, 3.5, and 6.0 are designated (AC, BC, KCR or KCO) - 2, (AC, BC, KCR or KCO) - 3, and (AC, BC, KCR or KCO) - 6, respectively. Extracted pectins at pH 2.0, 3.5 and 6.0 from apple, beet and two kiwifruit cell walls at pH 2.0, 3.5, and 6.0 are designated (AP, BP, KPR or KPO) - 2, (AP, BP, KPR or KPO) - 3, and (AP, BP, KPR or KPO) - 6, respectively.

**Table 1.** The common names of cell wall components, their abbreviations and their ATR-FTIR frequencies ($cm^{-1}$) determined with our spectrometer of the studied plant cell wall polysaccharides.

| | Sample names | Abbreviations | Linkable peaks or regions ($cm^{-1}$) |
|---|---|---|---|
| **Monosaccharides** | D-(-)-Arabinose | Ara | 1312, 1128*s*, 1088*s*, 1050***vs***, 991***vs***, 940, 890*s*, 841*s* |
| | D-(+)-Xylose | Xyl | 1146, 1123*s*, 1034***vs***, 1016*s*, 930*s*, 902*s* |
| | D-(+)-Mannose | Man | 1110*s*, 1064*s*,1034***vs***,1016***vs***, 966*s*, 949*s*, 912, 879 |
| | D-(+)-Galactose | Gal | 1154*s*, 1142, 1100*s*, 1056***vs***, 1039***vs***, 990, 971, 953*s*, 827*s* |
| | L-Rhamnose | Rha | 1375, 1290, 1226, 1145, 1116*s*, 1074*s*, 1026***vs***, 976*s*, 907, 874, 827*s* |
| | D-(+)-Glucose | Glc | 1228, 1206, 1150*s*,1100*s*, 1052*s*, 1016***vs***, 991***vs***, 912*s*, 840*s* |
| | D-(-)-Fucose | Fuc | 1334s, 1140s, 1095*s*, 1083***vs***, 1050***vs***, 976***vs***, 921, 868, 814 |
| | D(+)-Galacturonic acid monohydrate | Gal A | 1756*s*, 1708*s*, 1275, 1218, 1155, 1095***vs***, 1062***vs***, 1025***vs***, 823*s* |
| **β-glucans** | Microcrystalline cellulose | MCCE | 1640, 1428, 1367, 1320, 1308, 1200, 1160, 1052*s*, 1030***vs***, 988*s*, 893 |
| | Yeast β-glucan | YGLU | 1640, 1428, 1367, 1308, 1200, 1160, 1068*s*, 1030***vs***, 988*s*, 886 |
| | Curdlan (1,3-β-o-glucan) | CGLU | 1640, 1428, 1367, 1308, 1200, 1160, 1068*s*, 1030***vs***, 988*s*, 886 |
| **Hemicelluloses** | Rye Arabinoxylan (59% xylose) | ARHV | 1164, 1035***vs***, 983*s*, 890 |
| | Wheet Arabinoxylan (64% xylose) | AXMB | 1164, 1035***vs***, 983*s*, 890 |
| | Wheet Arabinoxylan (77% xylose) | AXLB | 1164, 1035***vs***, 983*s*, 890 |
| | Xylan (Beechwood) | XYBW | 1164, 1035***vs***, 983*s*, 890 |
| | 1,4-β-D-Mannan | MANB | 1367, 1065***vs***, 1035***s***, 1013***vs***, 938*s*, 890, 870*s*, 807*s* |
| | Galactomannan (Carob) | GAMA | 1065***vs***, 1027***vs***, 870*s*, 807*s* |
| | Xyloglucan (from tamarind seed) | XYGT | (1040-1010)***vs***, 939, 890 |
| | Xyloglucan Oligosaccharides | XYGO | (1040-1010)***vs***, 939, 890 |
| | Xyloglucan (Hepta-, +Octa, +Nona-saccharides) | XYGH | (1040-1010)***vs***, 939, 890 |
| **Pectins** | Citrus peel pectin | CPPC | 1740*s*, 1600, 1440, 1230, 1141, 1097*s*, 1014***vs***, 954, 914, 831 |

(Continued)

**Table 1.** (Continues)

| Sample names | Abbreviations | Linkable peaks or regions ($cm^{-1}$) |
|---|---|---|
| Commercial apple pectin | APPC | 1740*s*, 1600, 1440, 1230, 1141, 1097*s*, 1014***vs***, 954, 914, 831 |
| Arabinan (sugar beet) | ARSB | 1600, the region of (1100 - 950) |
| Linear 1,5-α-L-arabinan (sugar beet) | LNAR | 1208, 1115, 1086*s*, 1071*s*, 1043***vs***, 1022***vs***, 1004***vs***, 982***vs***, 948*s* |
| Debranched arabinan (sugar beet) | DBAR | 1600, 1208, 1115, 1086*s*, 1071*s*, 1043***vs***, 1022***vs***, 1004***vs***, 982***vs***, 948*s* |
| Galactan (Potato) | GTAN | 1600, 1405, 1039***vs***, 884*s* |
| Rhamnogalacturonan I (from potato pectic fibre) | RGPP | 1740, 1600***s***, 1410, 1238, 1141*s*, 1097*s*, 1074s, 1014***vs***, 954 |
| Rhamnogalacturonan (from soybean pectic fibre) | RGSP | 1600***s***, 1410, 1141*s*, 1097*s*, 1074s, 1014***vs***, 954 |
| Homogalacturonan DM 70 | HGTN | 1740***vs***, 1440, 1230, 1140, 1097*s*, 1014***vs***, 970*s*, 914 |
| Poly-galacturonic acid | GALN | 1590***s***, 1410*s*, 1330, 1141*s*, 1097*s*, 1014***vs***, 954*s* |

114 * IR band intensity: *vs*, very strong; *s*, strong.

## 2.2. Characterization of carbohydrate composition

Sugar analysis was performed as previously described by Liu et al. (2021). For neutral sugars analysis, 10 mg of cell walls or cellulose were submitted to a Saeman acid hydrolysis (Saeman, Moore, Mitchell, & Millett, 1954) and then to simple hydrolysis (dissolved in 1 mol/L sulfuric acid) whereas soluble polysaccharides (10 mg) were only submitted to simple hydrolysis. The derivatization to alditol acetates (Englyst, Wiggins, & Cummings, 1982) allows the detection of sugars by gas chromatography with a flame ionization detector (Agilent, Inc., Palo Alto, USA). Galacturonic acid was measured by a meta-hydroxyl-diphenyl assay (Blumenkrantz & Asboe-Hansen, 1973). The methanol was measured by a stable isotope dilution assay using headspace-GC-MS (QP2010 Shimadzu Kyoto, Japan) as described by Renard & Ginies (2009). The degree of methylation (DM) was then calculated as the molar ratio of methanol to galacturonic acid.

## 2.3. ATR-FTIR spectra

All cell wall polysaccharide samples, in the form of dry powder, were stored in $P_2O_5$ atmosphere before analysis to remove residual water. ATR-FTIR spectra data (4000 to 600 $cm^{-1}$) were acquired at room temperature in a Tensor 27 FTIR spectrometer (Bruker Optics®, Wissembourg, France), using a single-reflectance horizontal ATR cell (Golden Gate with a diamond crystal, Bruker Optics®) equipped with a system to press the dried homogenized samples on the crystal surface (Bureau et al. 2012). Each sample was analyzed three times (using after homogenization three

different aliquots of the powders) to consider its heterogeneity, and each spectrum was the average of 16 scans. Spectral pre-processing and data treatment using multivariate analyses were performed with MATLAB 7.5 (Mathworks Inc. Natick, MA) software using the SAISIR package (Cordella & Bertrand, 2014). The spectral data were pretreated with baseline correction and standard normal variate (SNV) to correct multiplicative interferences and variations in baseline shift before any multivariate analysis.

### 2.4. Statistical analysis

All biochemical analyses were presented as mean values of analytical triplicates and the reproducibility of the results was expressed as pooled standard deviations (Pooled SD). Pooled SD was calculated per series of replicates using the sum of individual variances weighted by the individual degrees of freedom (Box, Hunter, & Hunter, 1978). A PCA was applied on the ATR-FTIR spectra in the range between 1800 and 800 $cm^{-1}$ in order to study the repartition of the cellulose, hemicelluloses and pectins in a space according to their composition and absorption bands. Spectral data pre-processing and PCA were performed using MATLAB 7.5 (Mathworks Inc. Natick, MA) software using the SAISIR package (Cordella & Bertrand, 2014). HCA was performed using R software using FactoMineR (for computing) and factoextra (for visualizing the results) (R Core Team., 2014).

## 3. Results and discussion

### 3.1. Characteristic bands of cell wall polysaccharides in the ATR-FTIR spectra

157 The compositions of the 58 cell wall polysaccharides from extracted and
158 commercial origin were determined in this study by both, the classical methods (Table
159 2, see Liu et al., 2021 for cell walls and extracted pectins) and ATR-FTIR
160 spectroscopy (Table 1, Figure 1). Detailed peak positions and assignments of each
161 pure cell wall polysaccharide were limited to the specific bands in the range of
162 1800-800 $cm^{-1}$ (detected in solid or liquid form) in agreement with the previous
163 works (Canteri et al., 2019; Coimbra et al., 1998, 1999; Ferreira et al., 2001; Filippov
164 & Kohn, 1975; Gnanasambandam, R., Proctor, 2000; Kacurakova et al., 2000;
165 Kyomugasho, Christiaens, Shpigelman, Van Loey, & Hendrickx, 2015; McCann,
166 Hammouri, Wilson, Belton, & Roberts, 1992; Monsoor, Kalapathy, & Proctor, 2001;
167 Szymanska-Chargot et al., 2015; Szymanska-Chargot & Zdunek, 2013) and
168 summarized in Table 3. Strong absorption bands in this region corresponding to the
169 specific wavenumbers assigned to pectins (e.g., rhamnogalacturonan and
170 homogalacturonan), hemicelluloses (e.g., xyloglucan, mannan, galactomannan,
171 arabinoxylan and xylan) and cellulose (Figure 1), are detailed below.

**Table 2.** Composition of extracted cell walls and pectins from fruits and vegetables and commercial purified cellulose, hemicelluloses and pectin components (mg/g dry weight, except for degree of methylation expressed in %).

| Codes | Rha | Fuc | Ara | Xyl | Man | Gal | Glc | Gal A | MeOH | DM |
|---|---|---|---|---|---|---|---|---|---|---|
| **β-glucans** | | | | | | | | | | |
| MCCE | 3 | 0 | 0 | 17 | 13 | 0 | 861 | - | - | - |
| CGLU | 0 | 0 | 0 | 0 | 0 | 0 | 705 | - | - | - |
| YGLU | 0 | 0 | 0 | 10 | 6 | 0 | 650 | - | - | - |
| **Hemicelluloses** | | | | | | | | | | |
| GAMA | 0 | 0 | 5 | 0 | 776 | 190 | 7 | - | - | - |
| ARHV | 0 | 0 | 321 | 486 | 0 | 17 | 0 | - | - | - |
| AXMB | 1 | 0 | 288 | 693 | 0 | 7 | 5 | - | - | - |
| AXLB | 1 | 0 | 209 | 733 | 0 | 6 | 5 | - | - | - |
| XYBW | 12 | 0 | 6 | 716 | 0 | 10 | 8 | - | - | - |
| MANB | 0 | 0 | 0 | 0 | 960 | 18 | 8 | - | - | - |
| XYGT | 1 | 0 | 12 | 282 | 0 | 140 | 399 | - | - | - |
| XYGO | 3 | 0 | 37 | 287 | 0 | 123 | 515 | - | - | - |
| XYGH | 1 | 0 | 3 | 281 | 0 | 106 | 506 | - | - | - |
| **Commercial pectins** | | | | | | | | | | |
| CPPC | 20 | 1 | 21 | 4 | 0 | 138 | 33 | 535 | 74 | 73 |
| APPC | 12 | 0 | 20 | 8 | 1 | 88 | 63 | 564 | 77 | 79 |
| ARSB | 52 | 0 | 584 | 0 | 0 | 114 | 0 | 83 | - | - |
| LNAR | 25 | 0 | 841 | 0 | 0 | 78 | 0 | 51 | - | - |
| DBAR | 68 | 0 | 504 | 0 | 0 | 193 | 48 | 98 | - | - |
| GTAN | 51 | 0 | 23 | 4 | 0 | 628 | 9 | 79 | | |
| RGPP | 54 | 0 | 10 | 3 | 0 | 105 | 0 | 473 | - | - |
| RGSP | 81 | 64 | 21 | 120 | 0 | 96 | 0 | 403 | - | - |
| HGTN | - | - | - | - | - | - | - | 814 | 100 | 68 |
| GALN | - | - | - | - | - | - | - | 850 | 0 | 0 |
| *Pooled SD* | *1.0* | *0.3* | *8.3* | *7.0* | *5.8* | *2.3* | *8.6* | *4.0* | *2.5* | *3.2* |

Pooled SD: pooled standard deviation. Rha: rhamnose, Fuc: fucose, Ara: arabinose, Xyl: xylose, Man: mannose, Gal: galactose, Glc: glucose, Gal A: galacturonic acid, MeOH: methanol, DM: degree of methylation. Hemicelluloses (ARHV: Rye Arabinoxylan (59% Xylose), AXMB: Wheet Arabinoxylan (64% Xylose), AXLB: Wheet Arabinoxylan (77% Xylose), XYBW: Xylan (Beechwood), MANB: 1,4-β-D-Mannan, XYGT: Xyloglucan (from tamarind seed), XYGO: Xyloglucan Oligosaccharides, XYGH: Xyloglucan Oligosaccharides (Hepta-, +Octa, +Nona-saccharides), GAMA: Galactomannan (Carob)); Pectins (APPC: Apple pectin, CPPC: Citrus peel pectin, HGTN: Homogalacturonan DM 70, GALN: Polygalacturonic acid, DBAR: Debranched arabinan, ARSB: Arabinan, LNAR: Linear arabinan, RGPP: Rhamnogalacturonan I, RGSP: Rhamnogalacturonan, GTAN: Galactan (Potato)); β-glucans (MCCE: Microcrystalline cellulose, CGLU: 1,3-beta-o-glucan and YGLU: Yeast beta-glucan).

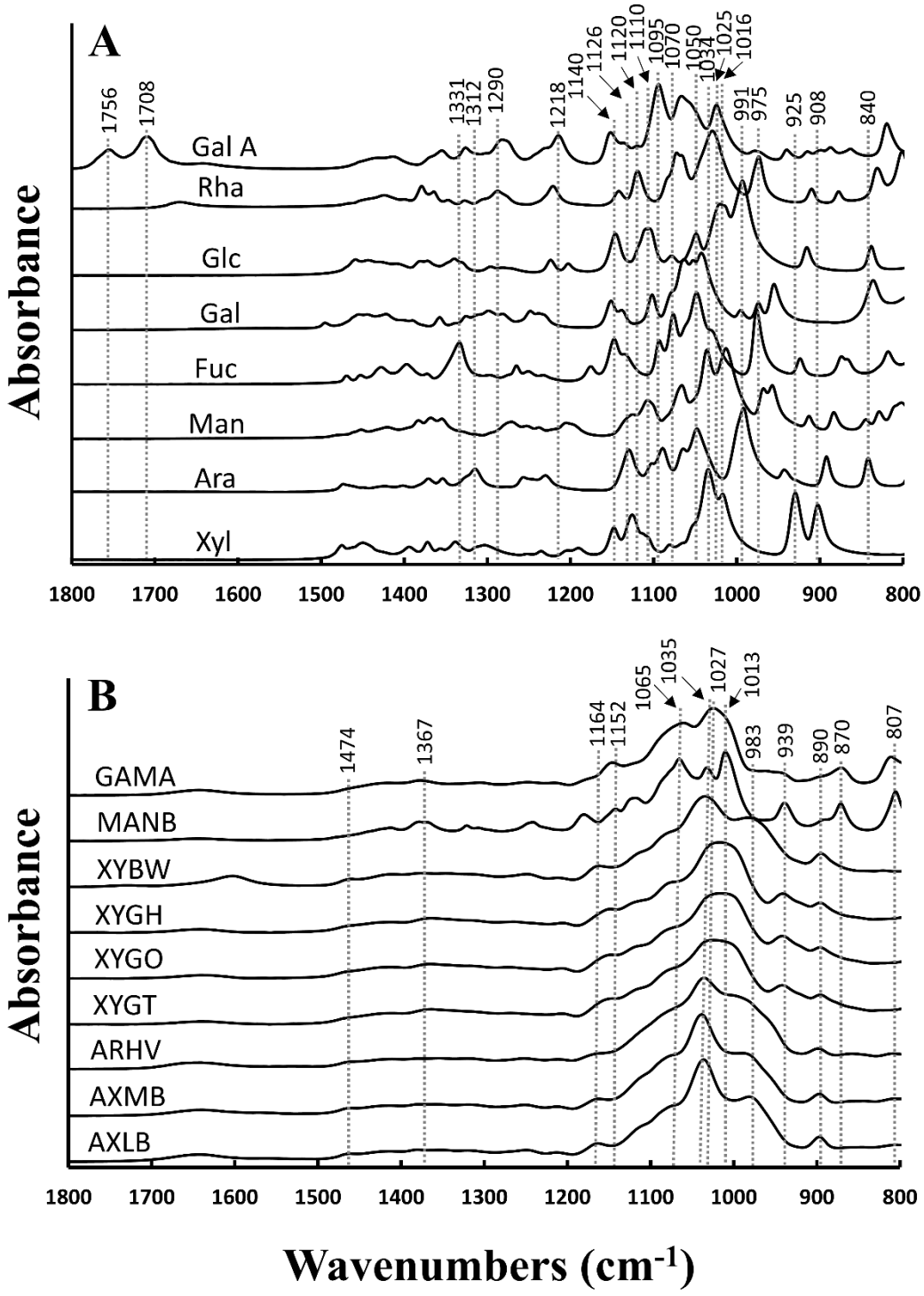
A
1756
1708
1331
1312
1290
1218
1140
1126
1120
1110
1095
1070
1050
1034
1025
1016
991
975
925
908
840
Gal A
Rha
Glc
Gal
Fuc
Man
Ara
Xyl
Absorbance
1800 1700 1600 1500 1400 1300 1200 1100 1000 900 800
B
1474
1367
1164
1152
1065
1035
1027
1013
983
939
890
870
807
GAMA
MANB
XYBW
XYGH
XYGO
XYGT
ARHV
AXMB
AXLB
Absorbance
1800 1700 1600 1500 1400 1300 1200 1100 1000 900 800
Wavenumbers (cm-1)

184

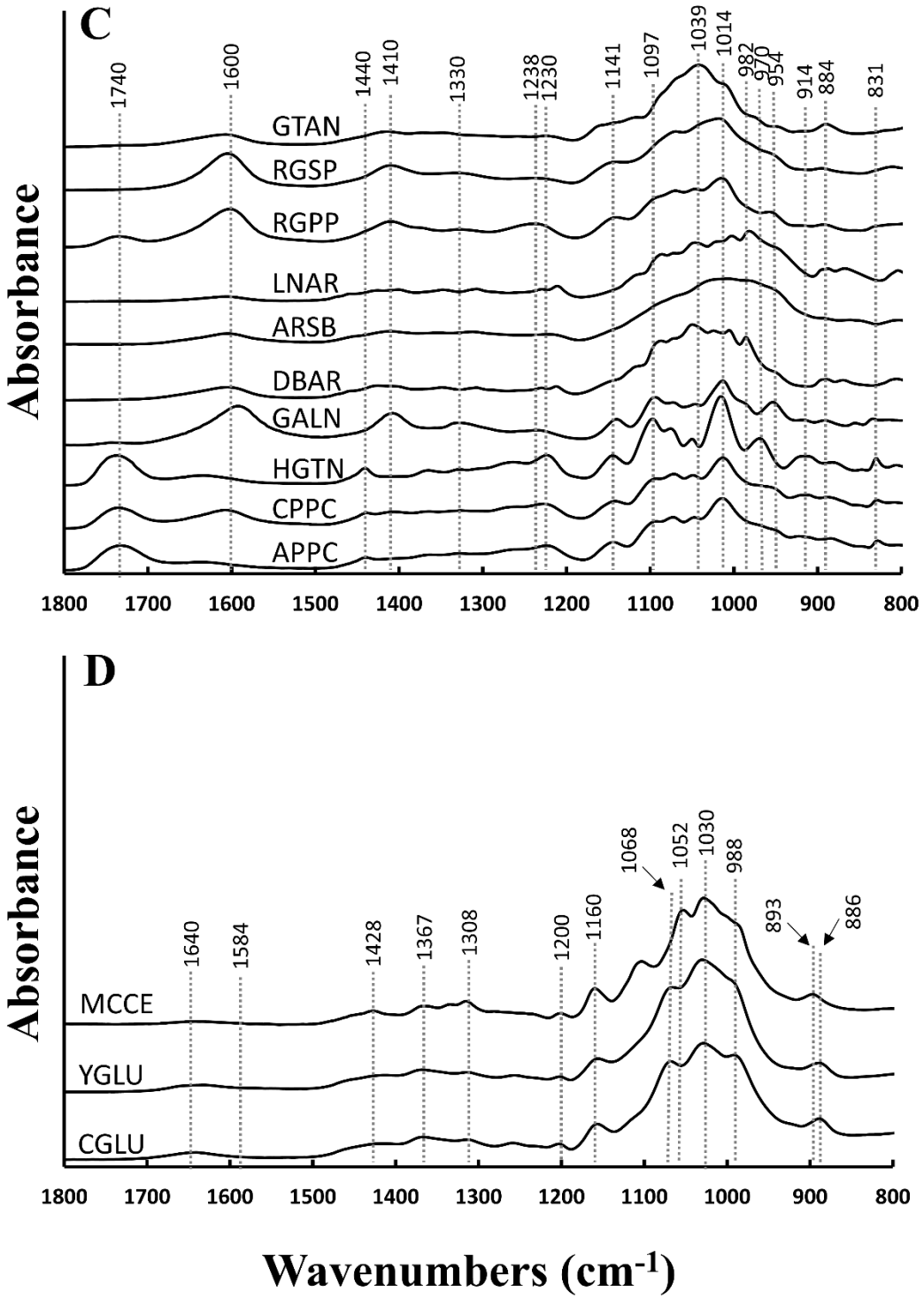


**Figure 1** ATR-FTIR spectra (pre-processed with Standard Normal Variate) of commercial purified and extracted cell wall polysaccharides in solid form: A. Monosaccharides (Rha: rhamnose, Fuc: fucose, Ara: arabinose, Xyl: xylose, Man: mannose, Gal: galactose, Glc: glucose, Gal A: galacturonic acid); B. Hemicelluloses (ARHV: Rye Arabinoxylan (59% Xylose), AXMB: Wheet Arabinoxylan (64% Xylose), AXLB: Wheet Arabinoxylan (77% Xylose), XYBW: Xylan (Beechwood), MANB: 1,4-β-D-Mannan, XYGT: Xyloglucan (from tamarind seed), XYGO: Xyloglucan Oligosaccharides, XYGH: Xyloglucan Oligosaccharides (Hepta-, +Octa, +Nona-saccharides), GAMA: Galactomannan (Carob)); C. Pectins (APPC: Apple pectin, CPPC: Citrus peel pectin, HGTN: Homogalacturonan DM 70, GALN: Polygalacturonic acid, DBAR: Debranched arabinan, ARSB: Arabinan, LNAR:

Linear arabinan, RGPP: Rhamnogalacturonan I, RGSP: Rhamnogalacturonan, GTAN: Galactan (Potato)); D. β-glucans (MCCE: Microcrystalline cellulose; CGLU: curdlan 1,3-beta-o-glucan; YGLU: Yeast beta-glucan).

196 **Table 3.** The main ATR-FTIR absorption bands, the polysaccharides in which they were detected and their tentative assignment. For polysaccharide identification (detailed in Table 1).

| **Wavenumber range ($cm^{-1}$) (detected)** | **Mono- or polysaccharide in which it was detected** | **Band assignments** | **Corresponding Wavenumber range ($cm^{-1}$)*** | **References** |
|---|---|---|---|---|
| 1756 & 1708 | Gal A | Galacturonic acid (absence of glycosidic bond) | - | - |
| 1740 | APPC, CPPC and HGTN | C=O stretching vibration of alkyl ester (pectin) | 1745-1730 | (Filippov & Kohn, 1975; Gnanasambandam, R., Proctor, 2000; McCann et al., 1992; Monsoor et al., 2001; Szymanska-Chargot & Zdunek, 2013) |
| 1640 | MCCE, CGLU and YGLU | H–O–H bending vibration absorbed water | 1640 | (Szymanska-Chargot et al., 2015) |
| 1605 - 1595 | GALN, CPPC, ARSB, DBAR, RGPP and RGSP | $COO^-$ antisymmetric stretching polygalacturonic acid, free carboxyl group | 1630-1600 | (Filippov & Kohn, 1975; Gnanasambandam, R., Proctor, 2000; McCann et al., 1992; Monsoor et al., 2001; Szymanska-Chargot & Zdunek, 2013) |
| 1525 | KCR/Os | Amid II N–H deformation (proteins); lignin and phenolic back bone | 1550 | (McCann et al., 1992) |
| 1474 | ARHV, XYBW and XYGT | Xylose-containing hemicellulose | - | - |
| 1440 | APPC, CPPC and HGTN | Asymmetric stretching modes vibration of methyl esters (pectin) | 1440 | (Canteri et al., 2019; Szymanska-Chargot et al., 2015) |
| 1428 | MCCE, CGLU and YGLU | $CH_2$ symmetric bending (cellulose) | 1428 | (Szymanska-Chargot & Zdunek, 2013) |
| 1410 | GALN, RGPP and RGSP | $COO^-$ symmetric stretching, free carboxyl group (rhamnogalacturonan and homogalacturonan) | 1410 | (Szymanska-Chargot & Zdunek, 2013) |
| 1367 | MCCE, CGLU and YGLU, XYGT, GAMA and MANB | C–H vibrations and $CH_2$ bending (cellulose, hemicelluloses) | 1370, 1362 | (Szymanska-Chargot et al., 2015; Szymanska-Chargot & Zdunek, 2013) |

(Continued)

**Table 3.** (Continues)

| Wavenumber range ($cm^{-1}$) (detected) | Mono- or polysaccharide in which it was detected | Band assignments | Corresponding Wavenumber range ($cm^{-1}$)* | References |
|---|---|---|---|---|
| 1331 | Fuc | Fucose (absence of glycosidic bond) | - | |
| 1330 | HGTN, GALN, RGPP and RGSP | Bending of O–H groups in pyranose ring of pectins | 1331-1320 | (Szymanska-Chargot et al., 2015; Szymanska-Chargot & Zdunek, 2013) |
| 1312 | Ara | Arabinose (absence of glycosidic bond) | - | |
| 1308 | MCCE, CGLU and YGLU | $CH_2$ symmetric bending or $CH_2$ rocking vibration (cellulose) | 1317-1313 | (Szymanska-Chargot et al., 2015; Szymanska-Chargot & Zdunek, 2013) |
| 1290 | Rha | Rhamnose (absence of glycosidic bond) | - | |
| 1238 | RGPP | Rhamnogalacturonan | - | |
| 1230 | APPC, CPPC and HGTN | C–O stretching (pectins) | 1240, 1230 | (Szymanska-Chargot et al., 2015; Szymanska-Chargot & Zdunek, 2013) |
| 1218 | Gal A | Galacturonic acid (absence of glycosidic bond) | - | - |
| 1164 | ARHV, XYBW and XYGT | Glycosidic bond vibrations (O–C–O) (xylose-containing hemicellulose) | 1173, 1153, 1147 | (Coimbra et al., 1999; Kacurakova et al., 2000) |
| 1160 | KCR/Os | Glycosidic bond vibrations (O–C–O) (cellulose in cell walls) | 1160 | (Canteri et al., 2019; Szymanska-Chargot & Zdunek, 2013) |
| 1152 | MANB and GAMA | Glycosidic bond vibrations (O–C–O) (mannose-containing hemicellulose) | 1150 | (Szymanska-Chargot et al., 2015) |
| 1141 | APPC, CPPC, GALN, HGTN, RGPP and RGSP | Glycosidic bond vibrations (O–C–O) (pectin) | 1150-1143 | (Coimbra et al., 1998, 1999) |
| 1126 | Ara | Arabinose (absence of glycosidic bond) | - | |

(Continued)

**Table 3.** (Continues)

| Wavenumber range ($cm^{-1}$) (detected) | Mono- or polysaccharide in which it was detected | Band assignments | Corresponding Wavenumber range ($cm^{-1}$)* | References |
|---|---|---|---|---|
| 1097 | APPC, CPPC, HGTN, GALN, RGPP and RGSP | C–O stretching, C–C stretching ring pectin | 1100-1090 | (Coimbra et al., 1998; Szymanska-Chargot et al., 2015; Szymanska-Chargot & Zdunek, 2013) |
| 1074 | GTAN, RGPP and RGSP | C–C stretching ring (galactan and rhamnogalacturonan) | 1072, 1070 | (Kacurakova et al., 2000) |
| 1068 | MCCE, CGLU and YGLU | C–O stretching, C–C stretching, C6–H2–O6 (cellulose) | 1059, 1047 | (Szymanska-Chargot et al., 2015) |
| 1065 | MANB and GAMA | C–O stretching, C–C stretching (mannose-containing hemicellulose) | 1064 | (Kacurakova et al., 2000) |
| 1039 | GTAN | C–C stretching ring (galactan) | 1038 | (Kacurakova et al., 2000) |
| 1035 | ARHV, XYBW and XYGT | C–O stretching, C–C stretching (xylose-containing hemicellulose) | 1042, 1041, 1038 | (Canteri et al., 2019; Coimbra et al., 1999; Kacurakova et al., 2000) |
| 1030 | MCCE, CGLU and YGLU | C–O stretching, C–C stretching, C6–H2–O6 (cellulose) | 1034, 1030 | (Kacurakova et al., 2000; Szymanska-Chargot & Zdunek, 2013) |
| 1027 | GAMA | C–O stretching, C–C stretching, C6–H2–O6 (galactomannan) | 1034 | (Kacurakova et al., 2000) |
| 1014 | APPC, CPPC, GALN, HGTN, DBAR, ARSB, GTAN, RGPP and RGSP | C–O stretching, C–C stretching pectin (C2–C3, C2–O2, C1–O1) backbone vibrations (pectin) | 1020, 1015, 1014 | (Coimbra et al., 1998, 1999; Szymanska-Chargot et al., 2015; Szymanska-Chargot & Zdunek, 2013) |
| 1013 | MANB | C–O stretching, C–C stretching (mannan) | - | |
| 991 | Glc and Ara | Glucose and arabinose (absence of glycosidic bond) | - | |
| 988 | MCCE, CGLU and YGLU | C–O stretching, C–C stretching cellulose (C6–H2–O6) | 1000, 985 | (Canteri et al., 2019; Szymanska-Chargot & Zdunek, 2013) |

(Continued)

**Table 3.** (Continues)

| Wavenumber range ($cm^{-1}$) (detected) | Mono or polysaccharide in which it was detected | Band assignments | Corresponding Wavenumber range ($cm^{-1}$)* | References |
|---|---|---|---|---|
| 983 | ARHV and XYBW | Xylan and arabinoxylan | - | |
| 982 | DBAR, ARSB and LNAR | Arabinan | - | |
| 970 | APPC, CPPC and HGTN | Pectins | 972 | (Kacurakova et al., 2000) |
| 954 | RGSP | CO bending (pectins) | 952 | (Coimbra et al., 1999; Szymanska-Chargot & Zdunek, 2013) |
| 939 | XYGT, GAMA and MANB | Ring vibration (hemicellulose and arabinan) | 941 | (Szymanska-Chargot et al., 2015; Szymanska-Chargot & Zdunek, 2013) |
| 925 and 908 | Xyl | Xylose (absence of glycosidic bond) | - | |
| 914 | APPC, CPPC, HGTN and GALN | Ring vibration (pectin) | - | |
| 890 | XYGT, ARHV and XYBW | C1–H bending (xylose-containing hemicellulose) | 893 | (Szymanska-Chargot & Zdunek, 2013) |
| 886 | KCR/Os | C1–H bending (cellulose) | 899, 895 | (Canteri et al., 2019; Szymanska-Chargot & Zdunek, 2013) |
| 884 | GTAN | C1–H bending (galactan) | 883 | |
| 870 | GAMA and MANB | C1–H bending (mannose-containing polysaccharide) | - | |
| 840 | Ara | Arabinose (absence of glycosidic bond) | - | |
| 831 | APPC, CPPC, GALN and HGTN | Ring vibration (pectin) | 833-830 | (Szymanska-Chargot et al., 2015; Szymanska-Chargot & Zdunek, 2013) |
| 807 | GAMA and MANB | Ring vibration (mannose-containing hemicellulose) | - | |

197 * Reference from the literatures. Monosaccharides (Rha: rhamnose, Fuc: fucose, Ara: arabinose, Xyl: xylose, Man: mannose, Gal: galactose, Glc: glucose, Gal A: galacturonic acid);

Hemicelluloses (ARHV: Rye Arabinoxylan (59% Xylose), AXMB: Wheet Arabinoxylan (64% Xylose), AXLB: Wheet Arabinoxylan (77% Xylose), XYBW: Xylan (Beechwood), MANB: 1,4-β-D-Mannan, XYGT: Xyloglucan (from tamarind seed), XYGO: Xyloglucan Oligosaccharides, XYGH: Xyloglucan Oligosaccharides (Hepta-, +Octa, +Nona-saccharides), GAMA: Galactomannan (Carob)); Pectins (APPC: Apple pectin, CPPC: Citrus peel pectin, HGTN: Homogalacturonan DM 70, GALN: Polygalacturonic acid, DBAR: Debranched arabinan, ARSB: Arabinan, LNAR: Linear arabinan, RGPP: Rhamnogalacturonan I, RGSP: Rhamnogalacturonan, GTAN: Galactan (Potato)); β-glucans (MCCE: Microcrystalline cellulose; CGLU: curdlan, 1,3-beta-o-glucan; YGLU: Yeast beta-glucan). Bands of monosaccharides such as mannose and galactose were not shown due to their overlapping with bands of polysaccharide polymers.

### 3.1.1. Monosaccharides

Monosaccharides, without any glycosidic linkage to other units, are the simplest component units of the cell wall polysaccharides, and have been shown to be important in polymer analysis and structure elucidation (Wiercigroch et al., 2017). It was necessary to consider here hexopyranoses (glucose, mannose and galactose), dehydro-hexopyranoses (rhamnose and fucose), pentopyranose (xylose), and pentofuranose (arabinose), standards with different positions of hydroxyl groups on C-2, C-3, and C-4 (Figure 1A). The spectra of pentoses (arabinose and xylose) were dominated by a band at 991 and 1034 $cm^{-1}$, respectively, mainly due to the $\nu$(C-C), $\nu$(C-O) and $\beta$(C-CH) vibrations (Edwards, 1976). For hexoses, D-(+)-glucose was observed by the main band at 991 $cm^{-1}$. D-(+)-galactose is almost identical in structure to D-(+)-glucose, with a different orientation in the C-4 OH group, but with a distinct spectral difference due to their free crystalline structure (Figure 1A). Similarly, the spectrum of other hexopyranoses with different hydroxyl group orientations on C-2, C-3, and C-4 was also significantly different. Therefore, the relative positions of (C-OH) essentially affected the spectrum through variations in their spatial arrangement and interactions. The detailed ATR-FTIR bands of monosaccharides with modes assignments are listed in Table 1.

### 3.1.2. Pectic components

Pectins are acidic hetero-polysaccharides mainly composed of homogalacturonan, rhamnogalacturonan I and II, and different neutral sugar side chains (e.g., arabinan

and galactan). The spectra of apple pectins (APPC) and citrus peel pectins (CPPC) had very similar characteristic bands (Figure 1C) centering at 1740, 1600, 1440, 1230, 1141, 1097, 1014, 954, 914 and 831 $cm^{-1}$. They have also similar levels of neutral sugars, galacturonic acid and degree of methylation (Table 2). The band at 1740 $cm^{-1}$ is assigned to the esterified galacturonic acids. This band is characteristic of pectins with a high degree of methylation (DM) such as high methylated homogalacturonan (DM=70) (HGTN). Inversely, the band of poly-galacturonic acid (GALN), which is non-esterified, was at 1600 $cm^{-1}$ due to the $COO^-$ carboxylate ion stretching. These two main characteristic bands of pectins are fixed and similar to those previously reported (Coimbra et al., 1999; Filippov & Kohn, 1975; Gnanasambandam, R., Proctor, 2000; Kacurakova et al., 2000; Reintjes, Musco, & Joseph, 1962; Szymanska-Chargot et al., 2015; Wojdyło, Figiel, Lech, Nowicka, & Oszmiański, 2014).

For a further interpretation of these spectra, pure pectic components were characterized in the same conditions. Notably, although these parts of the polysaccharide components were not a complete pectin structure found in the plant, they are representative of different subunits of the pectins. For rhamnogalacturonan (RGPP and RGSP), the band at 1014 $cm^{-1}$ was the strongest (Figure 1C). However, this peak overlapped with the main peak of commercial pectins (APPC and CPPC). Some other specific bands, assigned to rhamnogalacturonan (RGPP and RGSP) can be used such as 1410, 1238 and 1074 $cm^{-1}$. In fact, RGSP contained more xylose than RGPP (120 mg/g *vs* 3 mg/g respectively) (Table 2). Based on the maximum peak of

246 xylose at 1035 $cm^{-1}$ for RGSP, but not for RGPP (Figure 1C), 1035 $cm^{-1}$ may be used
247 to differentiate the abundance of xylose in cell wall polysaccharides.

248 In the case of the main neutral sugar side chains of pectins (Figure 1C): (i)
249 galactan (GTAN) was characterized by bands at 1039 $cm^{-1}$, 1014 and 884 $cm^{-1}$; and
250 (ii) arabinan, such as present in sugar beet arabinan (ARSB), linear arabinan (LNAR)
251 and debranched arabinan (DBAR), were more visible in the region between 1100 and
252 950 $cm^{-1}$. The arabinans with different linearity and branching degrees had some
253 minor peak intensity differences in this region. For example, the main band of LNAR
254 (with the highest arabinose content, Table 2) was close to 980 $cm^{-1}$, which may be
255 used to assess arabinan. However, the characteristic peaks of arabinan (sugar beet)
256 were in the region and also within the range of the main peaks of other pectins (e.g.,
257 commercial pectins, rhamnogalacturonan and galactan) not allowing a clear
258 assignment of bands between 1100 and 950 $cm^{-1}$. In aqueous solutions, Kacurakova et
259 al. (2000) observed bands at 1070 and 1043 $cm^{-1}$ for rhamnogalacturonan, 1072 $cm^{-1}$
260 for galactan and 1039 $cm^{-1}$ arabinan, which were too close for reliable discrimination.
261 These differences may be due to the different states (solid or solution) of the cell wall
262 compounds and probably also to the specificity of the used spectrometers.

263 For pectic homogalacturonans with more or less methylation, the main
264 characteristic peaks (especially 1740, 1600, 1097 and 1014 $cm^{-1}$) were stable
265 regardless of whether they are in a solid crystalline state or in an aqueous solution.
266 However, the identification of spectral characteristic peaks of arabinan, galactan, and

rhamnogalacturonan required caution as their peaks were dependent on the sample state, which could lead to their overlapping with those of hemicelluloses and pectins.

### 3.1.3. Hemicelluloses and cellulose

Bands at 1474, 1367, 1164, 1152, 1065, 1035, 1027, 1013, 983, 939, 890, 870 and 807 $cm^{-1}$ were identified for hemicelluloses (Figure 1B). Xylan (XYBW) had characteristic absorption bands at 1035 $cm^{-1}$ and 983 $cm^{-1}$. The arabinoxylans with different xylose contents (Table 2), e.g., ARHV (59%), AXMB (64%) and AXLB (77%), showed a main band at 1035 $cm^{-1}$ for which the intensity varied with the xylose content. Xyloglucan (XYGT, XYGO and XYGH) absorbed in the region of 1040-1010 $cm^{-1}$, like hemicelluloses and cellulose making it difficult to be identified. Galactomannan (GAMA) and mannan (MANB) had bands at 1027 and 1013 $cm^{-1}$, respectively. In addition, they had a common secondary band at 1065 $cm^{-1}$, and two specific peaks at 870 and 807 $cm^{-1}$ (also found in softwood sample, Simonović, Stevanic, Djikanović, Salmén, & Radotić, 2011), which allowed them to be distinguished from others (Figure 1B). Therefore, the bands which could be assigned to xylose- and mannose- containing hemicelluloses were 1474, 1164, 1035, 983 and 890 $cm^{-1}$ for xylose-, and 1152, 1065, 1027, 1013, 939, 870 and 807 $cm^{-1}$ for mannose-, respectively (Table 3). This was confirmed for xylose- containing hemicelluloses including XYBW, ARHV, AXMB, AXLB, XYGT, XYGO and XYGT, and mannose- containing hemicelluloses including MANB and GAMA.

The bands characteristic of cellulose, β-(1→4)-linked glucan, for MCCE, were at

1640, 1428, 1367, 1320, 1308, 1200, 1160, 1052, 1030, 988 and 893 $cm^{-1}$ (Figure 1D), whereas bands at 1068 and 886 $cm^{-1}$ (instead of 1052 and 893 $cm^{-1}$ ) were identified for β-(1→3)-glucans (YGLU and CGLU). These slight differences for two peaks may contribute to distinguish 1,3-β- and 1,4-β- bonds.

### 3.1.4. Glycosidic linkage

The glycosidic linkages are an important characteristic structure in polysaccharides and influence the spectral changes in aqueous solutions (Jockusch et al., 2004; Kačuráková & Mathlouthi, 1996; Kanou, Nakanishi, Hashimoto, & Kameokaj, 2005; Nikonenko, Buslov, Sushko, & Zhbankov, 2000; Wiercigroch et al., 2017). For example, the spectra of the glycosidic bonds with different positions and configurations of oligo- and poly- saccharides in aqueous solution differ markedly from monosaccharides, with stretching vibrations [ν(CO)] of the C-O-C glycosidic linkage being the marker of the polysaccharide configuration. These vibrations appear in the two spectral ranges 1160-1130 and 1000-960 $cm^{-1}$ (Kacurakova et al., 2000; Kačuráková & Mathlouthi, 1996; Wiercigroch et al., 2017). Similarly, these bands appear in cell wall polysaccharides in the solid states when compared with monosaccharides (Figure 1). For xylose units with β-(1→4) glycosidic linkage (XYBW) bands were found at about 1164 $cm^{-1}$, for glucose units with β-(1→4) glycosidic linkage (YGLU, CGLU and MCCE) bands were found at 1160 $cm^{-1}$ and for mannose units with β-(1→4) glycosidic linkage (MANB) bands were found at 1152 $cm^{-1}$. Bands at 1141 $cm^{-1}$ for pectins originate from the stretching motion of the

309 CO bond within the glycosidic linkage (Coimbra et al., 1999). Therefore, the
310 involvement of glycosidic bonds influenced the spectrum through changes in their
311 spatial arrangement, type and position.

312 However, some monosaccharides also showed spectral bands in the region
313 between 1100 to 1000 cm $^{-1}$ presenting overlapping with those of polysaccharides
314 (Figure1, Table 1).

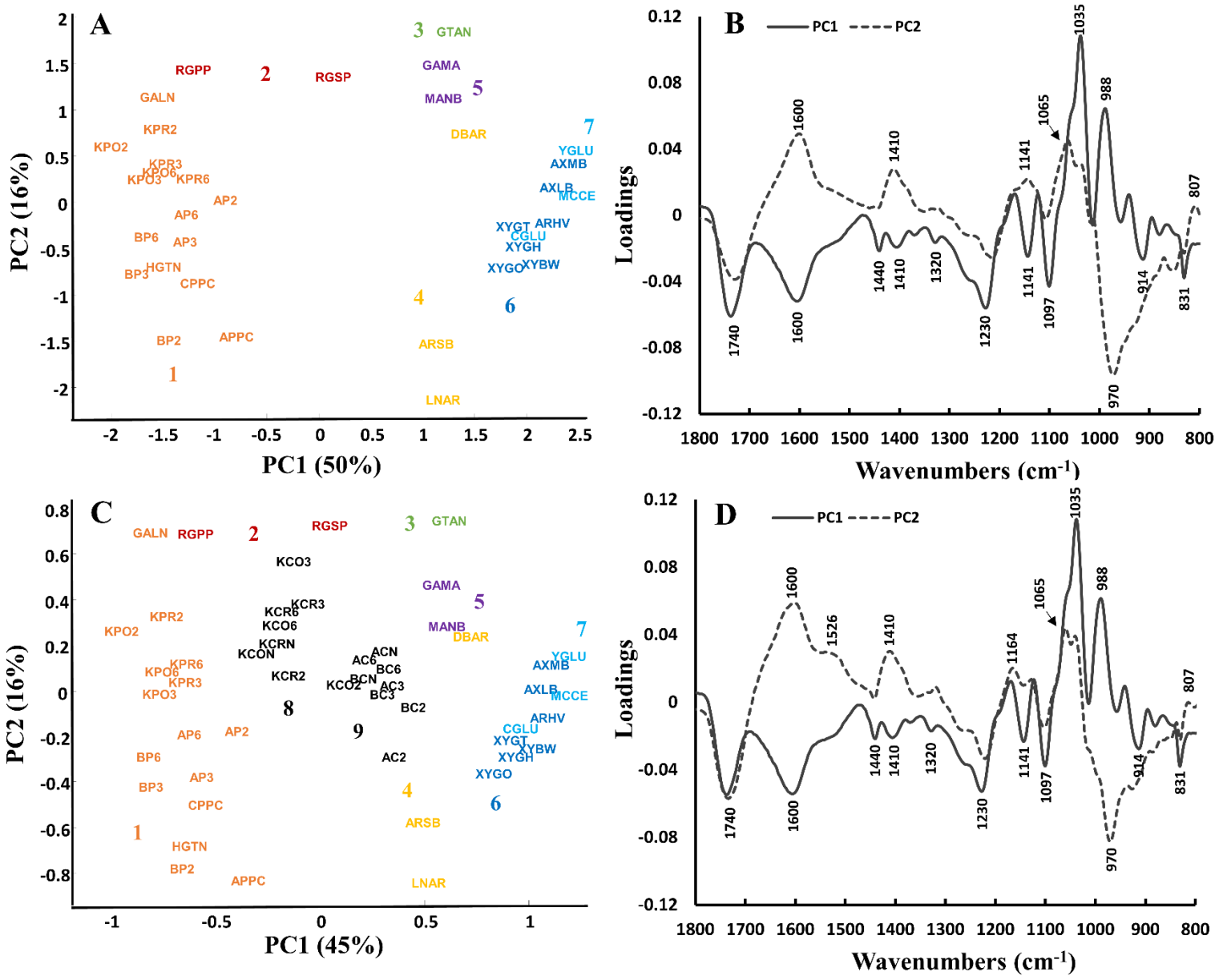
A
PC2 (16%)
PC1 (50%)
RGPP
RGSP
GTAN
GAMA
MANB
DBAR
GALN
KPR2
KPO2
KPR3
KPO6
KPO3
KPR6
AP2
AP6
BP6
AP3
HGTN
BP3
CPPC
BP2
APPC
ARSB
LNAR
YGLU
AXMB
AXLB
MCCE
XYGT
ARHV
CGLU
XYGH
XYGO
XYBW
1
2
3
4
5
6
7
B
PC1
PC2
Loadings
Wavenumbers (cm-1)
1740
1600
1440
1410
1320
1230
1141
1097
1065
1035
988
970
914
831
807
C
PC2 (16%)
PC1 (45%)
KCO3
KCR3
KCR6
KCO6
KCRN
KCON
KCR2
KCO2
ACN
AC6
BC6
BCN
AC3
BC3
BC2
AC2
8
9
D
PC1
PC2
Loadings
Wavenumbers (cm-1)
1600
1526
1410
1164
1065
1035
988
1440
1410
1320
1141
1097
1230
914
831
807
970



315

**Figure 2** PCA scores scatter plots of 1) commercial and extracted pectins, 2) rhamnogalacturonan, 3) galactan, 4) arabinan, 5) mannose- containing hemicelluloses, 6) xylose- containing hemicelluloses and 7) cellulose (A), and all cell wall materials (excluding monosaccharides): 8) kiwifruit cell walls, 9) apple and beet cell walls (C). ATR-FTIR spectra in the range 1800 to 800 $cm^{-1}$ with their PCA loading profile of components PC1 and PC2 (B) and (D). Monosaccharides (Rha: rhamnose, Fuc: fucose, Ara: arabinose, Xyl: xylose, Man: mannose, Gal: galactose, Glc: glucose, Gal A: galacturonic acid); Hemicelluloses (ARHV: Rye Arabinoxylan (59% Xylose), AXMB: Wheet Arabinoxylan (64% Xylose), AXLB: Wheet Arabinoxylan (77% Xylose), XYBW: Xylan (Beechwood), MANB: 1,4-β-D-Mannan, XYGT: Xyloglucan (from tamarind seed), XYGO: Xyloglucan Oligosaccharides, XYGH: Xyloglucan Oligosaccharides (Hepta-, +Octa, +Nona-saccharides), GAMA: Galactomannan (Carob)); Pectins (APPC: Apple pectin, CPPC: Citrus peel pectin, HGTN: Homogalacturonan DM 70, GALN: Polygalacturonic acid, DBAR: Debranched arabinan, ARSB: Arabinan, LNAR: Linear arabinan, RGPP: Rhamnogalacturonan I, RGSP: Rhamnogalacturonan, GTAN: Galactan (Potato)); β-glucans: (MCCE: Microcrystalline cellulose; CGLU: curdlan, 1,3-beta-o-glucan; YGLU: Yeast beta-glucan).

### 3.2. Discrimination of cell walls

Two multivariate analyses were used to study the discrimination of complex fruit cell walls in comparison with that obtained on standard compounds. A Principal component analysis (PCA) was carried out using the spectral data (Figure 2A) to identify the mapping of cell wall polysaccharides (excluding extracted cell walls and monosaccharides). PC1 and PC2 explained respectively 50% and 16% of the total variance. Along the PC1, the samples were well discriminated due to the different types of cell wall polysaccharides. Positive loadings of PC1 covered wavenumbers characteristic of xylose-containing (1035 $cm^{-1}$) hemicellulose and cellulose (988 $cm^{-1}$) (Figure 2B). The negative high values of PC1 were obtained for wavenumbers at 1740 and 1600 $cm^{-1}$ characteristic of esterified and non-esterified carboxyl groups in pectins (Figure 2B), respectively and of 1440, 1320, 1230, 1141, 1097, 914 and 831 $cm^{-1}$ bands characteristic of pectins (Figure 2B). In addition, negative PC1 loading appeared for wavenumbers at 1410 $cm^{-1}$ characteristic for rhamnogalacturonan. The PC2 separated the esterified pectins and arabinan on the negative side (at the bottom) from the less esterified pectins, galactan and mannose-containing hemicelluloses (at the top). The bands at (1600 and 1141 $cm^{-1}$), 1410 $cm^{-1}$, and (1065 and 807 $cm^{-1}$) were attributed to respectively free carbonyl group of pectins, rhamnogalacturonan and mannose-containing hemicelluloses with a positive correlation to PC2. The region closes to 1740 and 970 $cm^{-1}$ corresponded to the esterified pectins with a negative correlation to PC2.

345 The same approach was used on the extracted cell walls from apple, beet and
346 kiwifruit (Figure 2C). The cell wall polysaccharides were divided into nine groups: 1)
347 commercial and extracted pectins; 2) rhamnogalacturonans; 3) galactans; 4) arabinans;
348 5) mannose- containing hemicelluloses; 6) xylose- containing hemicelluloses; 7)
349 cellulose; 8) kiwifruit cell walls; 9) apple and beet cell walls. The first seven groups
350 are similar to Figure 2A, with the later addition of the extracted cell walls in the
351 center of the Figure 2C. This is consistent with the expected results as they contain
352 intact cell wall polysaccharide components. However, the extracted cell walls issued
353 from different species and extraction conditions were not well separated, especially
354 for apple and beet cell walls. How can we explain the lack of discrimination of cell
355 walls between apple and beet, whereas their composition differ significantly (Liu et
356 al., 2021)? As shown on the PCA, the kiwifruit cell walls were at the upper left in the
357 middle of the Figure 2C, while the apple and beet cell walls were at the bottom right
358 in the middle of the Figure 2C. This was probably linked to the high cellulose and
359 relatively low galacturonic acid for kiwifruit, and the high galacturonic acid for both
360 apple and beet (140 to 206 mg/g for apple, 141 to 225 mg/g for beet) (Liu et al., 2021).
361 However, the cell walls of apple and beet were not distinguished, in spite of marked
362 chemical and structural differences (Liu et al., 2021). Even a PCA performed on the
363 ATR-FTIR spectra of the cell walls of apple and beet alone did not separate them well
364 (data not shown). Beet cell walls are rich in arabinan (111 to 189 mg/g), contain
365 ferulic acid, and have only minor amounts of rhamnose, fucose, xylose and mannose.
366 Apple cell walls contain as much or more xylose (65 to 75 mg/g) and galactose (63

-67 mg/g) than arabinose (27 to 66 mg/g). However, the expected separation of apple and beet cell walls spectra by the characteristic peaks of arabinan (982 $cm^{-1}$) or galactan (1039 $cm^{-1}$) was not observed. Probably the characteristic peaks were not detected or were overlapped with those of other cell wall components, e.g., hemicelluloses or cellulose (Figure 1). This may be a limitation of ATR-FTIR in cell wall characterization, because arabinan and galactan are well known to change during ripening or processing.

PC loadings (Figure 2D) were very close to those obtained on the standard compounds (Figure 2B), probably reflecting the fact that the cell walls are by themselves combinations of pectins, hemicelluloses and cellulose. PC2 loadings had an extra shoulder peak at 1526 $cm^{-1}$, which may be attributed to lignin and ferulic acid, but occurring in combination with hemicelluloses (e.g., xylans and xyloglucans). The non-polysaccharide compounds in the cell wall, such as proteins (e.g., C = O of amides at 1655 $cm^{-1}$ and N-H of amides at 1540, and 1234 $cm^{-1}$), lignins (e.g., 1520, 1410 and 921 $cm^{-1}$) and other phenolic compounds (e.g., 1520, 1440, 1284, 1196 and 1075 $cm^{-1}$) have absorption bands which mare interfere with those of polysaccharides. This needs to be taken into account when characterizing cell walls using ATR-FTIR. Moreover, the structure of xylans varies with the source of the plant, such as wheat or beechwood. As an example, some phenolic compounds can couple beechwood xylan chains via ferulate dimerization (dehydrodiferulate cross-links) and/or incorporation into lignin, thus affecting their spectral bands (Kačuráková et al., 1999).

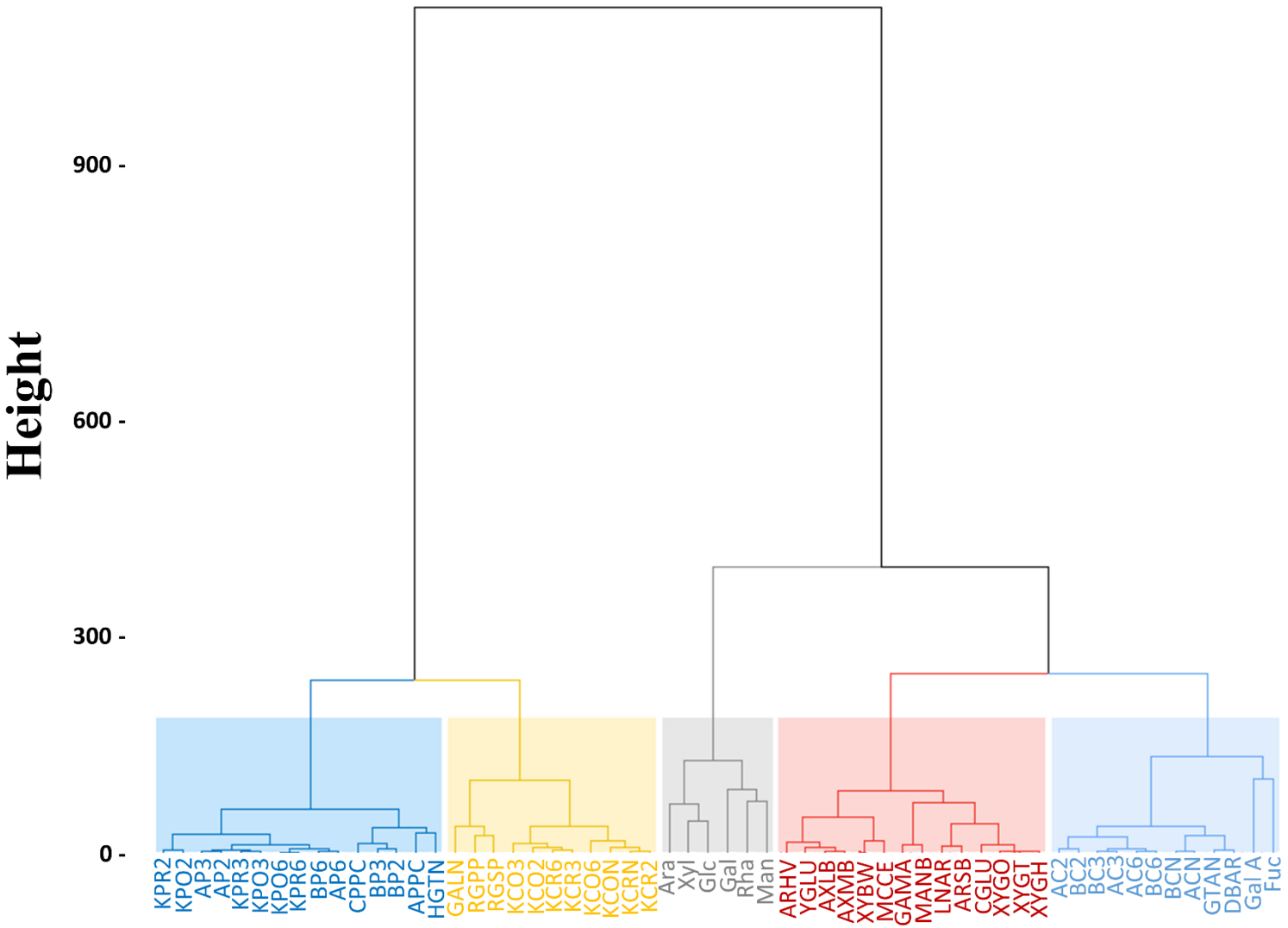
Height
900 -
600 -
300 -
0 -
KPR2
KPO2
AP3
AP2
KPR3
KPO3
KPO6
KPR6
BP6
AP6
CPPC
BP3
BP2
APPC
HGTN
GALN
RGPP
RGSP
KCO3
KCO2
KCR6
KCR3
KCO6
KCON
KCRN
KCR2
Ara
Xyl
Glc
Gal
Rha
Man
ARHV
YGLU
AXLB
AXMB
XYBW
MCCE
GAMA
MANB
LNAR
ARSB
CGLU
XYGO
XYGT
XYGH
AC2
BC2
BC3
AC3
AC6
BC6
BCN
ACN
GTAN
DBAR
Gal A
Fuc

388

**Figure 3** Hierarchical cluster analysis dendrogram of 58 cell wall and cell wall polysaccharide and monosaccharide samples based on average ATR-FTIR spectra in the range 4000 to 600 $cm^{-1}$ using Ward's clustering algorithm with Euclidian distance. From left to right, the groups are (i) commercial and extracted pectins; (ii) kiwifruit cell walls and RG; (iii) monosaccharides; (iv) cellulose and hemicelluloses and (v) apple and beet cell walls. Monosaccharides (Rha: rhamnose, Fuc: fucose, Ara: arabinose, Xyl: xylose, Man: mannose, Gal: galactose, Glc: glucose, Gal A: galacturonic acid); Hemicelluloses (ARHV: Rye Arabinoxylan (59% Xylose), AXMB: Wheet Arabinoxylan (64% Xylose), AXLB: Wheet Arabinoxylan (77% Xylose), XYBW: Xylan (Beechwood), MANB: 1,4-β-D-Mannan, XYGT: Xyloglucan (from tamarind seed), XYGO: Xyloglucan Oligosaccharides, XYGH: Xyloglucan Oligosaccharides (Hepta-, +Octa, +Nona-saccharides), GAMA: Galactomannan (Carob)); Pectins (APPC: Apple pectin, CPPC: Citrus peel pectin, HGTN: Homogalacturonan DM 70, GALN: Polygalacturonic acid, DBAR: Debranched arabinan, ARSB: Arabinan, LNAR: Linear arabinan, RGPP: Rhamnogalacturonan I, RGSP: Rhamnogalacturonan, GTAN: Galactan (Potato)); β-glucans: (MCCE: Microcrystalline cellulose; CGLU: curdlan, 1,3-beta-o-glucan; YGLU: Yeast beta-glucan).

Hierarchical cluster analysis (HCA) is widely applied as an unsupervised classification method to calculate distances between samples and cluster them according to this distance, based here on their spectra (Granato, Santos, Escher, Ferreira, & Maggio, 2018). HCA highlighted five groups (Figure 3). Group 1 clustered samples with high galacturonic acid contents from apple, beet, citrus and kiwifruit pectins. Group 2 contained samples with linear pectins and less side chains from kiwifruit cell walls, polygalacturonic acid and rhamnogalacturonan. Group 3 associated monosaccharide samples with absence of glycosidic bonds. Group 4 clustered samples including hemicelluloses and cellulose. Group 5 clustered samples with high methylated pectins and rich in arabinose and galactose, extracted from apple, beet cell walls, galactan and arabinan. Therefore, ATR-FTIR spectroscopy coupled with chemometrics allowed a good discrimination of cell walls related to their compositions and structures, giving some classes according to the different kinds of pectins, hemicelluloses and cellulose.

The cell walls represented a polymer system in a complex mixture with a diversity of both compositions and structures. PCA and HCA performed on the spectral data allowed to discriminate samples according to their cell wall polysaccharides. ATR-FTIR could be considered as a fast and easy way to distinguish different types of cell walls. Due to their complexity and the numerous spectral bands for each component, with the addition of overlapping, it was therefore difficult to assign each band to a compound chemical structure. However, the observed changes in intensity or presence/absence of some bands reflected the differences in

419 composition between the cell walls. And, slight changes in the strength and position
420 of individual bands could also be due to the different conformations of cell wall
421 polymers and the interactions between individual components.

422 **4. Conclusions**

423 ATR-FTIR spectra in the region between 1800 and 800 $cm^{-1}$ combined with PCA
424 has been widely applied to study the main polysaccharides present in the complex cell
425 walls. However, it is not always possible to analyze the structural changes in cell wall
426 polysaccharides at the molecular level and not all absorption bands allow
427 differentiation. Their complex structures, compositions, glycosidic linkage patterns
428 and the interactions between polysaccharides (or even with polyphenols and proteins)
429 make the application of ATR-FTIR to plant cell walls still challenging.

430 What can be determined is that: 1) xylan, arabinoxylan and xyloglucan all had the
431 same characteristic band at 1035 $cm^{-1}$; 2) cellulose showed a characteristic band at
432 988 $cm^{-1}$; 3) the mannan and galactomannan were identified by the bands at 1065 and
433 807 $cm^{-1}$; 4) the degree of methylation of pectin homogalacturonans was easily
434 determined by the relative height of the two bands at 1740 and 1600 $cm^{-1}$. According
435 to these results, the analysis of purified cell wall polysaccharides could be easily and
436 successfully performed directly with these bands giving information on the main cell
437 wall compounds: pectins, hemicelluloses and cellulose.

438 However, some difficulties remain to identify intact cell wall components and in
439 particular to discriminate cell walls of apple and beet in relation to the bands of

arabinan and galactan. The main chain made of arabinan did not give available characteristic peaks. The specific band of galactan at 1039 $cm^{-1}$ was overlapped with the bands of hemicelluloses. Therefore, the application of ATR-FTIR spectroscopy for the characterization of cell wall polysaccharides requires more in-depth research and should be used in combination with other analytical techniques.

**Acknowledgements**

LIU Xuwei would like to acknowledge China Scholarship Council (CSC) and Institut National de Recherche pour l'Agriculture, l'Alimentation, et l'Environnement (INRAE) for financial support to his PhD study.

## References


Anderson, C. T., & Kieber, J. J. (2020). Dynamic Construction, Perception, and Remodeling of Plant Cell Walls. *Annual Review of Plant Biology*, *71*(1), 39–69. https://doi.org/10.1146/annurev-arplant-081519-035846

Blumenkrantz, N., & Asboe-Hansen, G. (1973). New method for quantitative determination of uronic acids. *Analytical Biochemistry*, *54*(2), 484–489. https://doi.org/10.1016/0003-2697(73)90377-1

Brahem, M., Renard, C. M. G. C., Gouble, B., Bureau, S., & Le Bourvellec, C. (2017). Characterization of tissue specific differences in cell wall polysaccharides of ripe and overripe pear fruit. *Carbohydrate Polymers*, *156*, 152–164. https://doi.org/10.1016/j.carbpol.2016.09.019

Bureau, S., Ścibisz, I., Le Bourvellec, C., & Renard, C. M. G. C. (2012). Effect of sample preparation on the measurement of sugars, organic acids, and polyphenols in apple fruit by mid-infrared spectroscopy. *Journal of Agricultural and Food Chemistry*, *60*(14), 3551–3563. https://doi.org/10.1021/jf204785w

Burton, R. A., Gidley, M. J., & Fincher, G. B. (2010). Heterogeneity in the chemistry, structure and function of plant cell walls. *Nature Chemical Biology*, *6*(10), 724–732. https://doi.org/10.1038/nchembio.439

Canteri, M. H. G., Renard, C. M. G. C., Le Bourvellec, C., & Bureau, S. (2019). ATR-FTIR spectroscopy to determine cell wall composition: Application on a large diversity of fruits and vegetables. *Carbohydrate Polymers*, *212*, 186–196. https://doi.org/10.1016/j.carbpol.2019.02.021

Carpita, N., Sabularse, D., Montezinos, D., & Delmer, D. P. (1979). Determination of the pore size of cell walls of living plant cells. *Science*, *205*(4411), 1144–1147. https://doi.org/10.1126/science.205.4411.1144

Chylinska, M., Szymanska-Chargot, M., & Zdunek, A. (2016). FT-IR and FT-Raman characterization of non-cellulosic polysaccharides fractions isolated from plant cell wall. *Carbohydrate Polymers*, *154*, 48–54. https://doi.org/10.1016/j.carbpol.2016.07.121

Coimbra, M. A., Barros, A., Barros, M., Rutledge, D., & Delgadillo, I. (1998). Multivariate analysis of uronic acid and neutral sugars in whole pectic samples by FT-IR spectroscopy. *Carbohydrate Polymers*, *37*, 241–248. https://doi.org/10.1016/S0144-8617(98)00066-6

Coimbra, M. A., Barros, A., Rutledge, D. N., & Delgadillo, I. (1999). FTIR spectroscopy as a tool for the analysis of olive pulp cell-wall polysaccharide extracts. *Carbohydrate Research*, *317*(1–4), 145–154. https://doi.org/10.1016/S0008-6215(99)00071-3

Cordella, C. B. Y., & Bertrand, D. (2014). SAISIR: A new general chemometric toolbox. *TrAC - Trends in Analytical Chemistry*, *54*, 75–82. https://doi.org/10.1016/j.trac.2013.10.009

Edwards, S. L. (1976). *An Investigation of the Vibrational Spectra of the Pentose Sugars*. *Lawrence Univeristy*.

Englyst, H., Wiggins, H. S., & Cummings, J. H. (1982). Determination of the non-starch polysaccharides in plant foods by gas-liquid chromatography of constituent sugars as alditol acetates. *The Analyst*, *107*(1272), 307–318. https://doi.org/10.1039/an9820700307

Ferreira, D., Barros, A., Coimbra, M. A., & Delgadillo, I. (2001). Use of FT-IR spectroscopy to follow the effect of processing in cell wall polysaccharide extracts of a sun-dried pear. *Carbohydrate Polymers*, *45*(2), 175–182. https://doi.org/10.1016/S0144-8617(00)00320-9

Filippov, M. P., & Kohn, R. (1975). Determination of the esterification degree of carboxyl groups of pectin with methanol by means of infrared spectroscopy. *Chem. Zvesti*, *29*(1), 88–91. Retrieved from https://www.chempap.org/?id=7&paper=5409

Gnanasambandam, R., Proctor, A. (2000). Determination of pectin degree of esterification by diffuse reflectance. *Food Chemistry*, *68*, 327–332. https://doi.org/10.1016/s0308-8146(99)00191-0

Granato, D., Santos, J. S., Escher, G. B., Ferreira, B. L., & Maggio, R. M. (2018). Use

of principal component analysis (PCA) and hierarchical cluster analysis (HCA) for multivariate association between bioactive compounds and functional properties in foods: A critical perspective. *Trends in Food Science and Technology*, *72*, 83–90. https://doi.org/10.1016/j.tifs.2017.12.006

Jockusch, R. A., Kroemer, R. T., Talbot, F. O., Snoek, L. C., Çarçabal, P., Simons, J. P., … Von Helden, G. (2004). Probing the Glycosidic Linkage: UV and IR Ion-Dip Spectroscopy of a Lactoside. *Journal of the American Chemical Society*, *126*(18), 5709–5714. https://doi.org/10.1021/ja031679k

Kacurakova, M., Capek, P., Sasinkova, V., Wellner, N., & Ebringerova, A. (2000). FT-IR study of plant cell wall model compounds: pectic polysaccharides and hemicelluloses. *Carbohydrate Polymers*, *43*(2), 195–203. https://doi.org/10.1016/S0144-8617(00)00151-X

Kačuráková, M., & Mathlouthi, M. (1996). FTIR and laser-Raman spectra of oligosaccharides in water: Characterization of the glycosidic bond. *Carbohydrate Research*, *284*(2), 145–157. https://doi.org/10.1016/0008-6215(95)00412-2

Kačuráková, M., Wellner, N., Ebringerová, A., Hromádková, Z., Wilson, R. H., & Belton, P. S. (1999). Characterisation of xylan-type polysaccharides and associated cell wall components by FT-IR and FT-Raman spectroscopies. *Food Hydrocolloids*, *13*(1), 35–41. https://doi.org/10.1016/S0268-005X(98)00067-8

Kanou, M., Nakanishi, K., Hashimoto, A., & Kameokaj, T. (2005). Influences of monosaccharides and its glycosidic linkage on infrared spectral characteristics of disaccharides in aqueous solutions. *Applied Spectroscopy*, *59*(7), 885–892. https://doi.org/10.1366/0003702054411760

Kyomugasho, C., Christiaens, S., Shpigelman, A., Van Loey, A. M., & Hendrickx, M. E. (2015). FT-IR spectroscopy, a reliable method for routine analysis of the degree of methylesterification of pectin in different fruit- and vegetable-based matrices. *Food Chemistry*, *176*, 82–90. https://doi.org/10.1016/j.foodchem.2014.12.033

Lan, W., Renard, C. M. G. C., Jaillais, B., Leca, A., & Bureau, S. (2020). Fresh,

freeze-dried or cell wall samples: Which is the most appropriate to determine chemical, structural and rheological variations during apple processing using ATR-FTIR spectroscopy? *Food Chemistry*, *330*, 127357. https://doi.org/10.1016/j.foodchem.2020.127357

Le Bourvellec, C., & Renard, C. M. G. C. (2012). Interactions between polyphenols and macromolecules: Quantification methods and mechanisms. *Critical Reviews in Food Science and Nutrition*, *52*(3), 213–248. https://doi.org/10.1080/10408398.2010.499808

Liu, X., Le Bourvellec, C., & Renard, C. M. G. C. (2020). Interactions between cell wall polysaccharides and polyphenols: Effect of molecular internal structure. *Comprehensive Reviews in Food Science and Food Safety*, *19*(6), 3574–3617. https://doi.org/10.1111/1541-4337.12632

Liu, X., Renard, C. M. G. C., Rolland-Sabaté, A., Bureau, S., & Le Bourvellec, C. (2021). Modification of apple, beet and kiwifruit cell walls by boiling in acid conditions: Common and specific responses. *Food Hydrocolloids*, *112*. https://doi.org/10.1016/j.foodhyd.2020.106266

McCann, M. C., Hammouri, M., Wilson, R., Belton, P., & Roberts, K. (1992). Fourier transform infrared microspectroscopy is a new way to look at plant cell walls. *Plant Physiology*, *100*(4), 1940–1947. https://doi.org/10.1104/pp.100.4.1940

Monsoor, M. A., Kalapathy, U., & Proctor, A. (2001). Determination of polygalacturonic acid content in pectin extracts by diffuse reflectance Fourier transform infrared spectroscopy. *Food Chemistry*, *74*(2), 233–238. https://doi.org/10.1016/S0308-8146(01)00100-5

Nikonenko, N. A., Buslov, D. K., Sushko, N. I., & Zhbankov, R. G. (2000). Investigation of stretching vibrations of glycosidic linkages in disaccharides and polysaccarides with use of IR spectra deconvolution. *Biopolymers (Biospectroscopy)*, *57*(4), 257–262. https://doi.org/10.1002/1097-0282(2000)57:4<257::AID-BIP7>3.0.CO;2-3

R Core Team. (2014). A Language and Environment for Statistical Computing. *R*

565 *Foundation for Statistical Computing*, *2*. Retrieved from
566 http://www.r-project.org
567 Reintjes, M., Musco, D. D., & Joseph, G. H. (1962). Infrared Spectra of Some Pectic
568 Substances. *Journal of Food Science*, *27*(5), 441–445.
569 https://doi.org/10.1111/j.1365-2621.1962.tb00124.x
570 Renard, C. M. G. C. (2005). Variability in cell wall preparations: Quantification and
571 comparison of common methods. *Carbohydrate Polymers*, *60*(4), 515–522.
572 https://doi.org/10.1016/j.carbpol.2005.03.002
573 Renard, C. M. G. C., & Ginies, C. (2009). Comparison of the cell wall composition
574 for flesh and skin from five different plums. *Food Chemistry*, *114*(3), 1042–1049.
575 https://doi.org/10.1016/j.foodchem.2008.10.073
576 Saeman, J. F., Moore, W. E., Mitchell, R. L., & Millett, M. A. (1954). Techniques for
577 the determination of pulp constituents by quantitiative paper chromatography.
578 *Tappi Journal*, *37*(8), 336–343.
579 Simonović, J., Stevanic, J., Djikanović, D., Salmén, L., & Radotić, K. (2011).
580 Anisotropy of cell wall polymers in branches of hardwood and softwood: A
581 polarized FTIR study. *Cellulose*, *18*(6), 1433–1440.
582 https://doi.org/10.1007/s10570-011-9584-1
583 Szymanska-Chargot, M., Chylinska, M., Kruk, B., & Zdunek, A. (2015). Combining
584 FT-IR spectroscopy and multivariate analysis for qualitative and quantitative
585 analysis of the cell wall composition changes during apples development.
586 *Carbohydrate Polymers*, *115*, 93–103.
587 https://doi.org/10.1016/j.carbpol.2014.08.039
588 Szymanska-Chargot, M., & Zdunek, A. (2013). Use of FT-IR Spectra and PCA to the
589 Bulk Characterization of Cell Wall Residues of Fruits and Vegetables Along a
590 Fraction Process. *Food Biophysics*, *8*(1), 29–42.
591 https://doi.org/10.1007/s11483-012-9279-7
592 Watrelot, A. A., Le Bourvellec, C., Imberty, A., & Renard, C. M. G. C. (2013).
593 Interactions between pectic compounds and procyanidins are influenced by

methylation degree and chain length. *Biomacromolecules*, *14*(3), 709–718. https://doi.org/10.1021/bm301796y

Wiercigroch, E., Szafraniec, E., Czamara, K., Pacia, M. Z., Majzner, K., Kochan, K., … Malek, K. (2017). Raman and infrared spectroscopy of carbohydrates: A review. *Spectrochimica Acta - Part A: Molecular and Biomolecular Spectroscopy*, *185*, 317–335. https://doi.org/10.1016/j.saa.2017.05.045

Wojdyło, A., Figiel, A., Lech, K., Nowicka, P., & Oszmiański, J. (2014). Effect of Convective and Vacuum-Microwave Drying on the Bioactive Compounds, Color, and Antioxidant Capacity of Sour Cherries. *Food and Bioprocess Technology*. https://doi.org/10.1007/s11947-013-1130-8